

Test Beam Results from the CDF Plug Upgrade Calorimeter

G. Apollinari

Rockefeller University, New York, NY 10021

for the CDF Plug Upgrade Group ¹

This report describes the performance of the CDF Plug Upgrade calorimeter measured at the Fermilab Meson Beam line. A 60° section of the Electromagnetic and Hadronic calorimeters has been exposed to e^+ , π^+ and μ^+ beams. We determine an energy resolutions of $\sigma(E)/E = 15.5\% / \sqrt{E}$ for the Electromagnetic and $\sigma(E)/E = 78\% / \sqrt{E} \oplus 5.3\%$ for the Hadronic Calorimeters (E measured in GeV). The linearity in the response is within specifications. The uniformity of transverse response is 1.6% for e^+ and 2.3% for π^+ . The Shower Maximum Detector, instrumenting the EM calorimeter, provides a position resolution of 1 mm for e^+ energies above 50 GeV. The detector calibration system, based on a set of movable Cs^{137} sources, is able to track the energy scale at the level of $\sim 1 - 2\%$.

1 Introduction

In preparation for the next Tevatron $\bar{p}p$ collider run (Run II) scheduled to begin in 1999, an ambitious upgrade program of the Collider Detector at Fermilab (CDF) is underway. A major detector component is the Plug Upgrade Calorimeter [1], which will cover polar angles from 38° to 3° ($1.1 < |\eta| < 3.5$). ² This new calorimeter will replace the existing gas calorimeter, whose time response would have poorly matched the operational conditions of the

¹ Members of the following CDF institutions participate in the Plug Upgrade: Fermilab, Brandeis U., MSU, Rochester U., UCLA, Wisconsin U., Texas Tech U., Rockefeller U., Tsukuba U., Waseda U., KEK, Bologna U. and Udine U.

² The pseudorapidity η is defined as $\eta = -\ln[\tan(\theta/2)]$, where θ is the angle with respect to the beam direction.

Tevatron in Run II, when the time interval between bunch crossings may be as short as 132 nsec.

2 Detector Description

Figure 1 shows a cross section of the Upgraded Plug Calorimeter. The calorimeter is a sampling device consisting of an electromagnetic (EM) section [4] with shower position detection, followed by a hadronic (HAD) section [5]. In both sections the active elements are scintillator tiles read out by wavelength shifting (WLS) fibers embedded in the scintillator and spliced [2] to clear fiber.

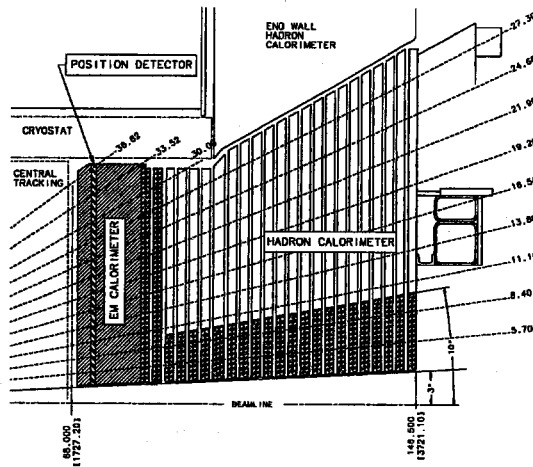


Fig. 1. Cross section of the upper part of the CDF Plug Upgrade Calorimeter

The active elements are arranged in towers pointing at the interaction vertex to provide the transverse segmentation. The size of the towers is approximately $0.1 \times 7.5^\circ$ in $\eta - \phi$ space. This segmentation achieves a reasonable compromise between the requirement of good efficiency in the e^\pm identification in semileptonic decays of b/\bar{b} jets and the constraints on the total number of channels.

The technical parameters and design specifications for the HAD and EM calorimeters are listed in table 1. The scintillator tiles of the first layer of the EM section are made out of 10 mm thick scintillator, are read out by Multi-Anode Photo-Multiplier Tubes (MAPMT) [3] and will act as preshower detectors. A Shower Maximum Position Detector (SMD) is located at the depth of the EM shower maximum (approximately $6 X_0$).

The optical systems for the EM, HAD and SMD are very similar. The scintillator elements are tiles (EM,HAD) or strips (SMD). They are cut from a large sheet of scintillator, and are assembled in triangularly shaped units called

	EM	HAD
Segmentation	$\sim 8 \times 8 \text{ cm}^2$	$\sim 24 \times 24 \text{ cm}^2$
Total Channels	960	864
Thickness	$21 X_0, 1 \lambda_0$	$7 \lambda_0$
Density	$0.36 \rho_{Pb}$	$0.75 \rho_{Fe}$
Samples	22 + Preshower	23
Active	4 mm SCSN38	6 mm SCSN38
Passive	4.5 mm Pb	2 inch Fe
Light Yield (pe/MIP/tile)	≥ 3.5	≥ 2
Non-linearity	$\leq 1 \%$	5-10 %
Resolution	$16\%/\sqrt{E} \oplus 1\%$	$80\%/\sqrt{E} \oplus 5\%$

Table 1
 Technical parameters and design specifications of the Plug Upgrade Calorimeter. The EM (HAD) resolution is for a single electron (pion).

megatiles. The megatiles are installed into *pizza pans* that provide top and bottom optical covers and also protect the optical assembly. The pizza pans are installed into the mechanical support provided by the absorbing material. Clear optical fiber cables connect to mass connectors on the outer edges of the pizza pans [7] and carry the light to the rear face of the plugs. There the optical cables plug into *decoder boxes*, which change the grouping of fibers from a layer-like to a tower-like geometry. The fiber groups coming from each tower are read out by PMTs connected to the decoder boxes and kept in a temperature-controlled environment. This optical path is shown schematically in figure 2.

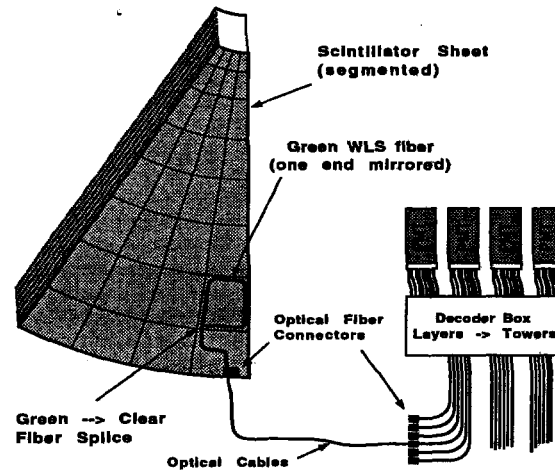


Fig. 2. Scheme for the light transmission from the scintillator tiles to the PMTs in the CDF Plug Upgrade Calorimeter.

A characteristic of this calorimeter is its high modularity. This modularity has

proven extremely useful during the construction phase, allowing the rejection and replacement of bad units, since every optical element of the calorimeter has been subject to Quality Assessment (QA) and Quality Control (QC) procedures to insure the construction of a detector satisfying the technical specifications (table 2). Moreover the calorimeter modularity greatly facilitates the final assembly, allowing the delicate step of optical cables installation to be kept separate from all the other steps of the detector assembly.

	Calorimeter Specification	Tile-Fiber Requirements
EM	$\sigma(E)/E$ Stoch. Term $\sim 16\%$ $\sigma(E)/E$ Const. Term $\leq 1\%$ Non-lin. $\leq 1\%$ (10-400 GeV)	Light Yield ≥ 3 p.e./MIP/Tile $\sigma_{UNIF} < 2.5\%$ $\sigma_{TOWER} < 10\%$
HAD	$\sigma(E)/E$ Stoch. Term $\sim 80\%$ $\sigma(E)/E$ Const. Term $\leq 5\%$	Light Yield ≥ 2 p.e./MIP/Tile $\sigma_{UNIF} < 4\%$ $\sigma_{TOWER} < 10\%$

Table 2

Requirements on the Tile/Fiber performances to achieve the Calorimeter Specifications. The requirements were determined using a GEANT simulation.

A system of Cs^{137} movable radioactive sources [6] exposes each tile (or strip) of the entire apparatus to radiation during the construction phase, to assure QC. Moreover the wire source system provides an anchor point for the energy scale determination. A laser system [8] is used to monitor the stability of the PMTs and digitization chain and a system of heat-exchangers controls and stabilizes the PMTs environment temperature.

A large “carbon copy” of the Plug Upgrade calorimeter has been assembled for test beam studies. All the technical solutions used in the final calorimeter have been implemented in this module to acquire a real-life experience. The module consists of a 60° azimuthal section of the full plug and it has been mounted on a precisely controlled movable table to allow the exposure of all its towers to the beam. The module has been tested with e^+ (5-120 GeV), π^+ (5-220 GeV) and μ^+ . The particle momentum and position of incidence on the face of the calorimeter is determined by a set of single wire drift chambers which provide an extrapolation precision of ~ 0.2 mm and a momentum precision of $\sim 0.2\%$. A removable preshower detector mounted in front of the Test Beam module is used to reject e^+ contamination in the π^+ studies. All PMTs and MAPMTs are read out using custom CDF electronics, which have been described elsewhere [9].

3 Preliminary Test Beam Results

Figure 3 shows a lego plot of the EM calorimeter response to one 50 GeV e^+ . The energy is shared among few towers, in agreement with expectations. The impact position of the e^+ as determined by the SMD is marked.

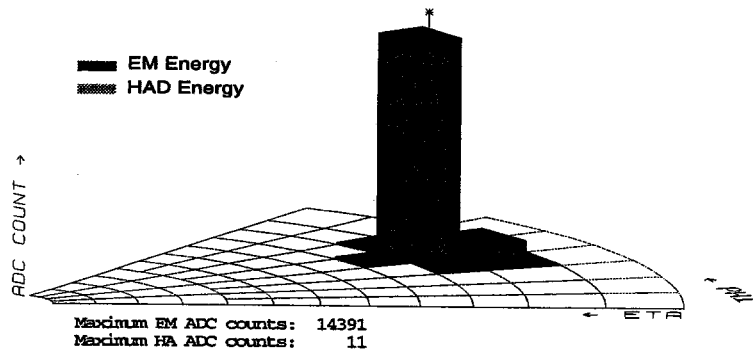


Fig. 3. Lego plot of the Test Beam module response to e^+ . The small tick on the tower response indicates the e^+ position measured by the SMD.

The relative energy resolutions are displayed in figure 4 for both e^+ and π^+ . They all agree with the design specifications. A study performed inserting $\sim 1 X_0$ of material in front of the detector to simulate the real operating conditions in CDF provided a constant term of $\sim 0.8\%$.

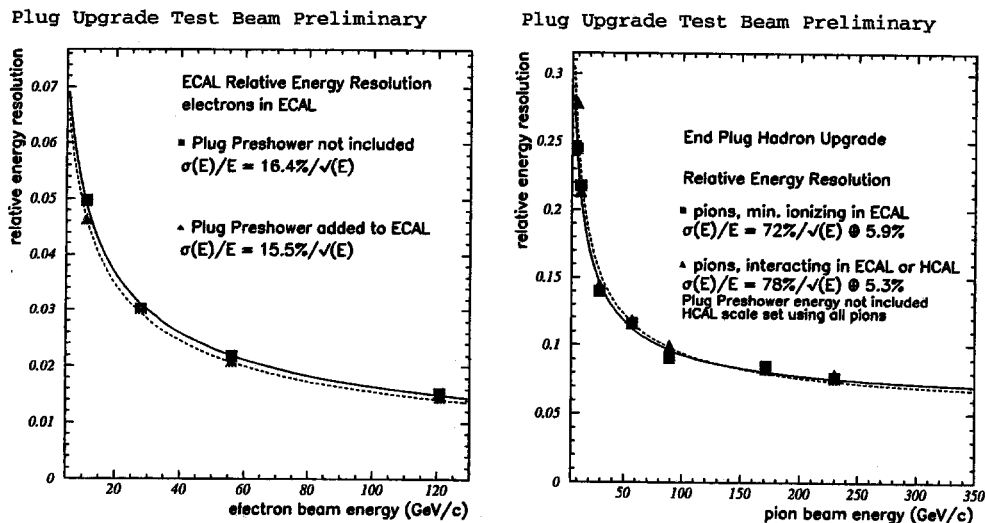


Fig. 4. Relative energy resolution for e^+ (left) and π^+ (right). The symbol \oplus indicates a sum in quadrature.

The relative linearity of response is shown in figure 5. The EM linearity satisfies the design requirements down to energies of $\sim 10 - 20$ GeV. We observe a $\sim 2\%$ non-linearity at 5 GeV. A similar non-linearity is expected at low

energies from our GEANT simulation. The HAD linearity reflects the non-compensating nature of the hadronic calorimeter. Both sections are also able to identify μ at equivalent energies of ~ 0.3 GeV and ~ 2 GeV.

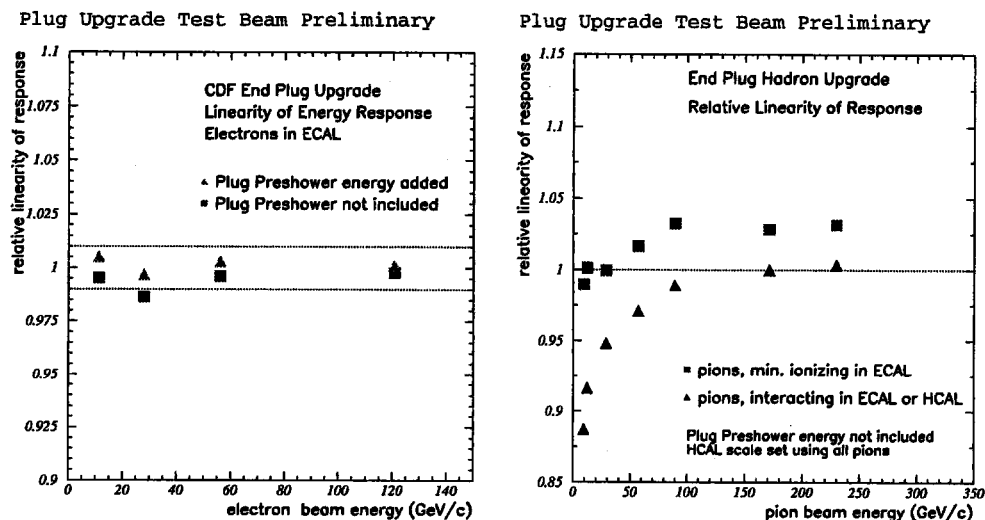


Fig. 5. Relative linearity for e^+ (left) and π^+ (right).

After the equalization of the PMT responses, the spread in the tower responses to e^+ and μ^+ is $\sim 5\%$. This number illustrates the tower uniformity obtained at construction time as a result of the program of QC and QA. The Cs^{137} is used subsequently for a further equalization of the response of the different towers. Figure 6 shows the correlation between the response of the towers to the Cs^{137} excitation and to 55 GeV e^+ . The spread of $\sim 1.8\%$ is an indication of the level of response uniformity we can achieve with this technology.

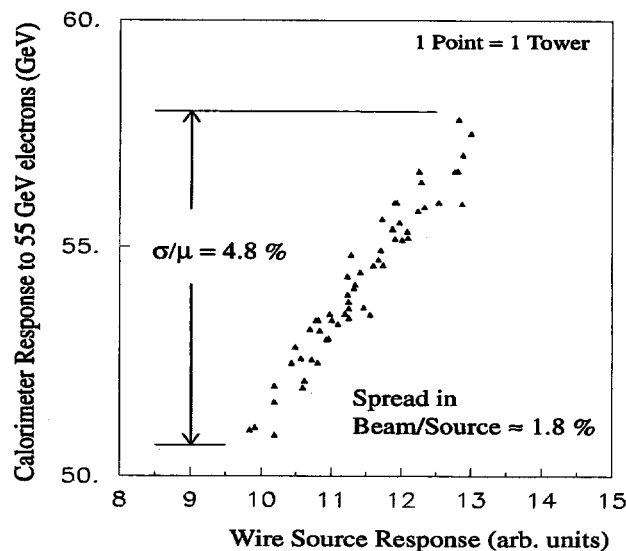


Fig. 6. Correlation between the response of the calorimeter towers to e^+ and to the radioactive source.

The uniformity in transverse response is shown in figure 7. For this study, the

detector is scanned by moving the module in small steps to achieve a uniform illumination over the face of a tower. The beam chambers accurately determine the position of incidence of the particles. The EM calorimeter transverse uniformity shows 4 *cold* spots corresponding to the vertex where 4 towers meet. The response in the *cold* spots is only 5 % below the average response. There are a couple of *warm* spots where the response is 5% higher than the average. The *warm* spots corresponds to positions in the scintillator where the WLS fiber is located. The spread in transverse uniformity for the EM calorimeter is 1.6 %. The HAD calorimeter does not show *warm* or *cold* spots due to the transverse size of hadronic showers. We measure a HAD transverse uniformity of 2.3%.

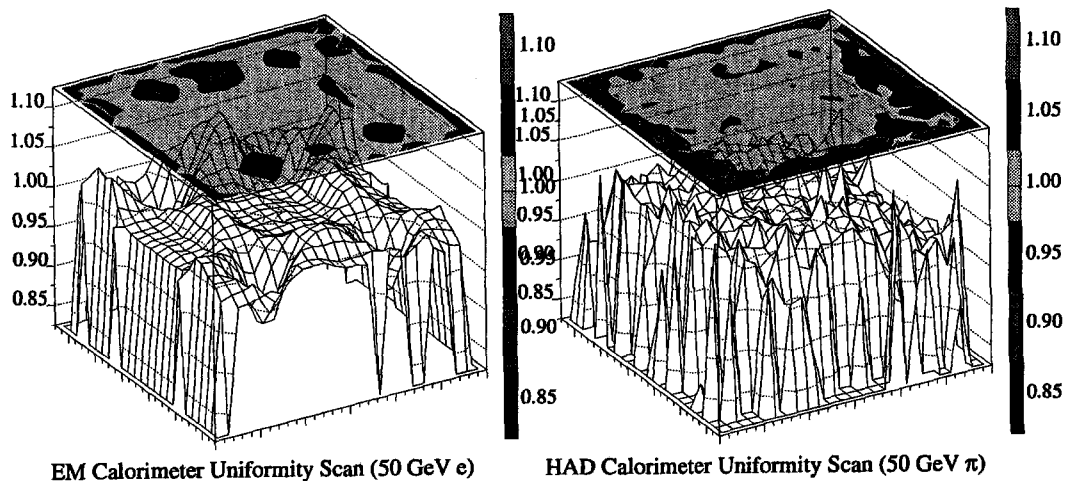


Fig. 7. Transverse response uniformity for e^+ in the EM (left) and π^+ in the HAD (right).

Figure 8 shows a schematic drawing of the SMD described briefly previously. 400 5 mm-wide scintillator strips are arranged in 45° sections. The strips are arranged parallel to one side of the section and there are two layers to provide an $\eta - \phi$ determination of an electromagnetic shower position. The strips are read-out individually by a WLS fiber connected to a pixel of a MAPMT. Since the SMD determines the shower position by interpolating the response of the strips illuminated by the shower, the strip responses must be equalized. The source tubes shown in figure 8 are essential to provide this equalization, given the relatively large intrinsic pixel-to-pixel gain variation in commercially available MAPMTs [3]. Also shown in figure 8 is the event display of a typical electromagnetic shower profile as seen by the SMD. The profile is narrow and contained mostly in 2-3 strips, in agreement with our GEANT simulation.

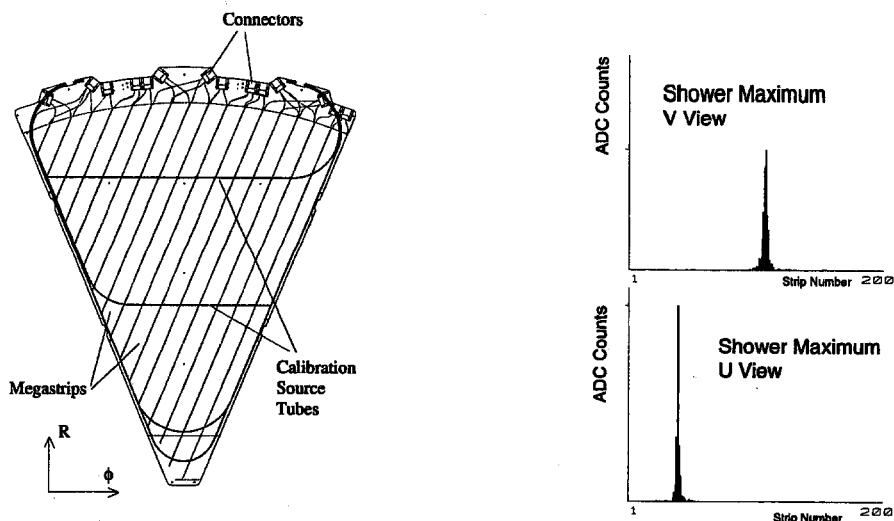


Fig. 8. Shower Maximum Detector module. Each megastrip is made by 10 individual, 5 mm wide strips (left). Typical electromagnetic shower profile measured by the SMD (right).

The correlation we observe between the strip response to the wire source and to e^+ has a spread of 5 % in the SMD. This implies that by equalizing the strips using the wire source, the technical requirement of a 10 % spread in the strip-to-strip equalization [10] is amply satisfied. A preliminary measurement of the position resolution is also shown in figure 9

Shower Max Phi and R Resolution vs. Beam Momentum

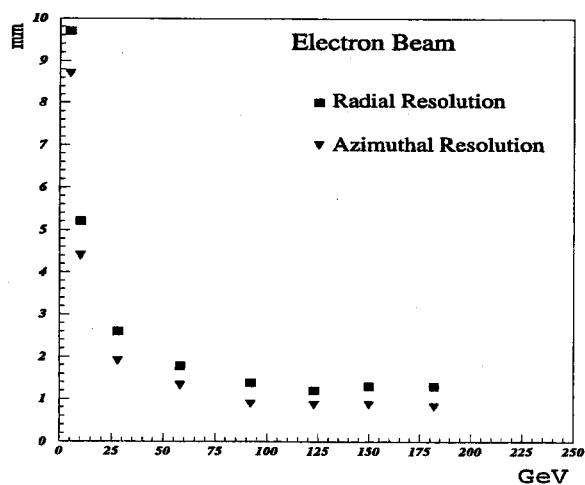


Fig. 9. SMD position resolution in the orthogonal views $r - \phi$ as a function of the e^+ energy.

4 Conclusion

The Plug Upgrade Calorimeter has been built over a period of 4 years with a very strict set of QC and QA procedures. The first test beam results show that these procedures allowed the assembly of a detector satisfying all the original technical requirements. We determine energy resolutions of $\sigma(E)/E = 15.5\%$

$1/\sqrt{E}$ and $\sigma(E)/E = 78\% / \sqrt{E} \oplus 5.3\%$ in the EM and HAD respectively, good linearity and very good transverse uniformity. The SMD position resolution is ~ 1 mm and the wire-source and laser systems are proving to be essential for the commissioning and calibration of the detector.

References

- [1] G. Apollinari *et al.*, in Proceedings of the Fourth International Conference on Calorimetry in High Energy Physics, La Biodola, Italy, edited by A. Menzione *et al.* (World Scientific, Singapore, 1993), p. 200
- [2] J. P. Mansour *et al.*, in Proceedings of the Workshop on Scintillating Fiber Detectors, Notre Dame, Indiana, edited by A. D. Bross *et al.* (World Scientific, Singapore, 1993), p. 534
G. Apollinari *et al.*, Nucl. Instr. Methods A **311**, 520 (1992)
- [3] Y. Bonushkin *et al.*, Nucl. Instr. Methods A **381**, 349 (1996) and references therein
- [4] T. Asakawa *et al.*, Nucl. Instr. Methods A **340**, 458 (1994)
S. Aota *et al.*, Nucl. Instr. Methods A **352**, 557 (1995)
- [5] P. de Barbaro *et al.*, IEEE Trans. Nucl. Sci. **42**, 510 (1995)
- [6] V. Barnes *et al.*, in Proceedings of the First International Conference on Calorimetry in High Energy Physics, Batavia, Illinois, edited by D. F. Anderson *et al.* (World Scientific, Singapore, 1990), p. 189
- [7] R. Bossert, in Proceedings of the Workshop on Scintillating Fiber Detectors, Notre Dame, Indiana, edited by A. D. Bross *et al.* (World Scientific, Singapore, 1993), p. 334
- [8] D. Cauz *et al.*, in Proceedings of the Sixth International Conference on Calorimetry in High Energy Physics, Frascati, Italy, edited by A. Antonelli *et al.* (Frascati Physics Series, 1996), p. 369
- [9] G. Drake *et al.*, Nucl. Instr. Methods A **269**, 68 (1988).

[10] P. Melese, in *Proceedings of the Workshop on Scintillating Fiber Detectors*, Notre Dame, Indiana, edited by A. D. Bross *et al.* (World Scientific, Singapore, 1993), p. 265